IN-02
380 368
DATE OVERRIDE

NASA

TECHNICAL MEMORANDUM
X - 25

EFFECT OF MULTIPLE-JET EXITS ON THE BASE PRESSURE

OF A SIMPLE WING-BODY COMBINATION AT

MACH NUMBERS OF 0.6 TO 1.27

By James M. Cubbage, Jr.

Langley Research Center
Langley Field, Va.

Declassified August 22, 1962

NATIONAL AERONAUTICS AND SPACE ADMINISTRATION

WASHINGTON   August 1959

NATIONAL AERONAUTICS AND SPACE ADMINISTRATION

TECHNICAL MEMORANDUM X-25

EFFECT OF MULTIPLE-JET EXITS ON THE BASE PRESSURE

OF A SIMPLE WING-BODY COMBINATION AT

MACH NUMBERS OF 0.6 TO 1.27

By James M. Cubbage, Jr.

SUMMARY

An investigation has been conducted at Mach numbers of 0.6 to 1.27 to determine the effect of multiple-jet exits on the base pressure of a simple wing-body combination. The design Mach number of the nozzles ranged from 1 to 3 at jet exit diameters equal to 36.4 to 75 percent of the model thickness. Jet total-pressure to free-stream static-pressure ratios ranged from 1 (no flow) to 34.2.

The results show that the variation of base pressure coefficient with jet pressure ratio for the model tested was similar to that obtained for single nozzles in bodies of revolution in other investigations. As in the case for single jets the base pressure coefficient for the present model became less negative as the jet exit diameter increased. For a constant throat diameter and an assumed schedule of jet pressure ratio over the speed range of these tests, nozzle Mach number had only a small effect on base pressure coefficient.

INTRODUCTION

The use of a clustered side-by-side jet engine installation - as opposed to the individual nacelle-type installation - in some supersonic aircraft designs has raised some question as to the effect on base and boattail drag of several jets operating in close proximity to each other. Although numerous investigations have dealt with the effect of a single jet on afterbody drag, the extent to which these effects may be modified by interjet and internacelle interference of multiple-jet installations has only recently received attention. (See refs. 1 to 4, for example.) Although primary interest for the multiple-jet installation lies in the

high supersonic speed range, the base drag at transonic speeds of some
configurations may be so large that acceleration through this speed
range may not be possible with the thrust available.

In order to aid in the establishment of the magnitude of jet effects
on afterbody drag for side-by-side multijet engine installations at tran-
sonic and low supersonic speeds, the jet effect program in progress at
the Langley Research Center was extended to include a general research
model with this type of jet installation. The model of this investiga-
tion consisted of a delta outer wing panel having 70° of leading-edge
sweep and a wall-mounted, rectangular cross-section body housing three
jet exits. The jet nozzles had exit Mach numbers of 1, 2, and 3 with
throat diameters of 1/2 inch and 3/8 inch. These nozzles were operated
at ratios of jet total pressure to free-stream static pressure from 1
(no flow) to about 34 over a free-stream Mach number range of 0.6 to
1.27. The effect of nozzle extension, two-jet operation, and wing panel
on base pressure was also investigated. The Reynolds number range for
this investigation was from 3.4×10^6 per foot to 4.9×10^6 per foot.

SYMBOLS

A area

$C_{D,b}$ base drag coefficient, $-\bar{C}_{p,b}\left(\dfrac{A_b - A_j}{A_{max}}\right)$

$C_{p,b}$ base pressure coefficient, $\dfrac{\frac{p_b}{p_\infty} - 1}{\frac{\gamma}{2} M_\infty^2}$

$\bar{C}_{p,b}$ average base pressure coefficient

D drag

d diameter

F thrust

M Mach number

p static pressure

p_t total pressure

$\dfrac{p_{t,j}}{p_\infty}$ jet pressure ratio; ratio of jet total pressure to free-stream static pressure

q dynamic pressure, $\dfrac{1}{2}\rho V^2$

V velocity

w mass-flow rate

γ ratio of specific heats

ρ mass density

ϵ nozzle half-angle; positive when diverging in direction of flow from center line of nozzle

Subscripts:

b base

i ideal; conditions for a fully expanded nozzle

j jet

max maximum

t throat

∞ free stream

o stagnation conditions

APPARATUS AND METHODS

Model and Nozzle Configurations

The model used in this investigation is shown in the photographs and drawing of figure 1. A sharp-edge inlet was incorporated in the model to reduce tunnel blockage and interference problems. This inlet was connected to a pump which provided a means of controlling the inlet velocity ratio. A simulated delta-wing panel with a leading-edge sweep-back angle of 70° was made from 1/8-inch-thick flat aluminum stock. The rear part of the nozzle housing was built up of plastic covering the nozzles and the 3/4-inch O.D. piping connecting the nozzles to the plenum chamber. (See fig. 1(b).) This assembly formed the main support point

for the cantilevered model. The plenum chamber was connected to three 1,000-cubic-foot-capacity tanks pressurized to approximately 325 pounds per square inch.

All nozzle configurations (fig. 2) with the exception of configuration 2A were tested in the base configuration shown in figures 1(a) and 1(b). Nozzle 2A was tested in the modified base shown in the upstream view of the model in figure 1(c). This base configuration was obtained by filling the boattailed areas between the nozzles with plastic so that the cross section of the model center section was constant throughout its entire length.

The nozzles, both sonic and supersonic types, were made up of conical sections. All nozzles except configurations 1A and 2A had the same throat diameter (0.364 inch); thus the same jet mass flow was kept for these nozzles at a given jet total pressure. In order to simulate two-engine operation, the center nozzle was replaced with a blank plug that was flush with the base of the model.

Tests were also made with the nozzles extended 1/8 inch beyond the base. Because of the method of constructing the model and nozzles it should be noted that in extending the nozzles a second base area is created around the jet exit. Since this second base area was part of the nozzle itself (see fig. 2) a base-pressure orifice could not be installed. Therefore, the magnitude of the base pressure on this annulus was not determined.

Tunnel

A side view of the $8\frac{1}{2}$ - inch by 12-inch slotted tunnel used in this investigation is shown in the photograph of figure 3. In this photograph the model mounting plate that replaced one window of the tunnel is shown together with the pipe connections for inlet air removal and jet supply air. The tunnel is a continuous operating type and is described in detail in reference 5. (For the present tests the inlet bell was free of all struts.) The maximum stagnation pressure of this tunnel was about $1\frac{3}{8}$ atmospheres at a stagnation temperature of 160° F.

Instrumentation and Methods

Instrumentation of the model consisted of nine base-pressure orifices, a static-pressure tap in the jet plenum chamber, and a total-pressure probe that was capable of traversing across the horizontal diameter of all three nozzles. A tenth base-pressure orifice on the partially boattailed model configuration became inoperative during tests

so that its pressure reading was not recorded. In addition to the pressure orifices on the model, orifices were installed in the mounting plate above and below the model. Visual observation of the flow by schlieren or shadowgraph methods was not made because of the method of mounting the model and the limited field of view through the opposite window. Total-pressure profiles obtained from the traversing probe showed that the jet flow for all three nozzles was symmetrical in the horizontal plane for all configurations except nozzles 1A and 2A (d_t = 0.50 inch). The asymmetry for these two nozzles was small, however, and was judged to be acceptable for this investigation.

In order to determine whether velocity gradients existed across the model and thus affected the base pressure, a spanwise row of static-pressure orifices was installed on the center section of the model 1 inch upstream of the base. In addition, the traversing probe was modified to measure total pressures above and below the model in the plane of the base. The spanwise Mach number distributions thus obtained were constant within $\pm 0.01 M_\infty$. This result was consistent with tunnel-empty axial Mach number distributions. (See ref. 5.) In addition, it was determined that the maximum deviation of the Mach number over the rear part of the model from the mean tunnel Mach number was 0.02.

With the exception of the tunnel stagnation pressure and the jet plenum chamber pressure, data were recorded photographically from multiple-tube manometer boards filled with tetrabromoethane. The tunnel stagnation pressure was read from a mercury U-tube manometer and the jet pressure in the plenum chamber was measured by a Bourdon type gage.

Profiles from the traversing total-pressure probe were recorded by two 2-variable recording potentiometers. At nominal Mach numbers of 0.6, 0.9, 1.0, 1.1, 1.2, and 1.26, data were recorded for several settings of the jet plenum chamber pressure; the corresponding total pressure at the throat of the nozzle was obtained from a calibration made previous to these tests. From repeat tests on the same configuration, it was determined that for identical test conditions base pressure coefficients could be repeated within ± 0.004.

RESULTS AND DISCUSSION

Effect of Jet Pressure Ratio on Base Pressure Coefficient

Base pressures measured by the individual orifices are presented in coefficient form in figure 4 as a function of jet pressure ratio $p_{t,j}/p_\infty$ for the three basic nozzles of this investigation. A rear view of the model is shown at the top of the figure to identify the orifice location

with the curve symbol. These data are typical of those obtained for the other nozzle configurations.

Under the pumping action of the jet the base pressure coefficient in figure 4 decreases (becomes more negative) as the jet pressure ratio is increased until under the favorable interference effects of the jet and external flow the base pressure coefficient increases with jet pressure ratio. This variation of $C_{p,b}$ in the vicinity of the jets with jet pressure ratio is similar to that obtained for single jets issuing from bodies of revolution. (See, for example, refs. 5 and 6.) Although the base-pressure-coefficient variation for each orifice in figure 4 follows a similar pattern, the range of coefficients for a given nozzle and jet pressure ratio is generally very large. For example, at $M_\infty = 1.0$ and $p_{t,j}/p_\infty = 5$ in figure 4(a), $C_{p,b}$ ranges from -0.230 to -0.530. However, it will be noted that this wide variation in base pressure coefficient tends to disappear at the higher jet pressure ratios and Mach numbers. For nozzles 1 and 2 at the highest Mach number the difference in the base pressure coefficients at the various orifices tends to increase again above a jet pressure ratio of about 15.

In order to facilitate comparison of the configurations, an arithmetic average base pressure coefficient $\overline{C}_{p,b}$ was computed for each nozzle configuration. (See figs. 5 to 9.) When this average was computed, the two orifices next to the tunnel wall (circle and square symbols in fig. 4) were omitted since this part of the model was intended only to place the jets outside the influence of boundary layer on the tunnel wall, and the pressure at the inoperative orifice was assumed to be equal to that measured by the orifice directly below it (diamond symbol in fig. 4). The average base pressure coefficients thus obtained for the three basic nozzles are presented in figure 5. It will be noted in this figure that the minimum value of $\overline{C}_{p,b}$ for the three nozzle configurations is approximately the same at sonic speeds and above and that, as M_∞ increases, the jet pressure ratio at which this minimum value of $\overline{C}_{p,b}$ occurs decreases. This result is consistent with results presented in references 3 and 5.

Effect of Nozzle Exit Diameter on Base Pressure

Figure 6 presents the average base pressure coefficient obtained for sonic nozzles, with two different jet diameters. (The curve for $d_j/d_b = 0.364$ is the same as that given in fig. 5(a).) The jet-pressure-ratio range is smaller for the larger nozzle ($d_t = 0.500$ inch) because of a larger pressure drop in the supply lines from the increased mass-flow rate.

The larger sonic jet results in a much more rapid variation in the base pressure than was observed for the smaller nozzle. This result is consistent with results from reference 5 and others. The minimum base pressure was greater (less negative) for the larger nozzle than for the smaller nozzle. Since the base area was also less for the larger nozzle, the reduction in maximum base drag would be correspondingly greater. It will be noted from the slope of the curves that positive base pressure coefficients would be expected in the jet-pressure-ratio range of about 15 to 22.

<center>Effect of Boattailing Between Nozzles for the</center>

<center>No-Jet Flow Condition</center>

The average base pressure coefficient obtained for the modified base configuration with nozzles 2A installed are shown in figure 7. With the jets operating this configuration is not directly comparable with any other configurations of this investigation since it was designed primarily to approximate the larger jet configurations of references 1 and 2. However, for the no-jet flow condition a comparison may be made between figure 7 and any configuration of figures 5 and 6 to determine the effect on base pressure of boattailing between nozzles. This comparison shows that $C_{p,b}$ was considerably smaller (more negative) for the filled-base configuration. This result would indicate that even a small amount of boattailing between nozzles is desirable insofar as base pressures are concerned.

<center>Effect of One Jet Inoperative on Base Pressure</center>

The data presented in figure 8 show the effect on average base pressure coefficient of closing off the middle jet; data for nozzle 1A are shown in figure 8(a) while data for nozzle 2 are shown in figure 8(b). In these two configurations the base was continuous between the two operating jets; that is, the space normally occupied by the middle jet was sealed. In general, for both configurations the inoperative nozzle is seen to increase $\overline{C}_{p,b}$ at the minimum-value point and to cause a reduction in the rate of increase of $\overline{C}_{p,b}$ as the jet pressure ratio increases above the minimum-value point. An increase in the minimum base pressure coefficient would be expected for the two-jet configurations as the aspiration effect of the jets would be less than that for the three-jet configurations. The maximum improvement in base pressure coefficient associated with loss of a supersonic nozzle (fig. 8(b)) at $M_{\infty} \approx 1.0$ was on the order of 40 percent as opposed to a maximum gain of approximately 25 percent when a sonic nozzle (fig. 8(a)) was removed. At other

Mach numbers and jet pressure ratios, the changes in base pressure coefficient were smaller.

Effect of Limited Nozzle Extension on Base Pressure

Data presented in reference 4 showed a reduction in base drag of cylindrical afterbodies with nozzles extended beyond the plane of the base. In order to determine the effect of nozzle extension on the base pressure coefficients of the present model, the $M_j = 2.0$ nozzle was extended 1/8 inch beyond the base. The average base pressure coefficients obtained on this configuration are presented in figure 9; for ease of comparison, the data presented previously (fig. 5(b)) are repeated in figure 9.

Extending the nozzles 1/8 inch had only a small effect on base pressure; however, it was generally beneficial over the jet-pressure-ratio range. Since the nozzle extension used was small compared with the nozzle diameter, it would be expected on the basis of data from reference 4 that a greater extension of the nozzles would show a corresponding improvement in base pressure.

Effect of Wing Panel on Base Pressure Coefficient

In figure 10 data are presented for the $M_j = 2.0$ nozzle with and without the wing panel attached to the center body. Except at $M_\infty = 1.01$, only a small difference is noted between the two configurations. The greater difference at $M_\infty = 1.01$ may result from the change in tunnel wall interference associated with addition of the wing; these effects, although present at other speeds, would reach their maximum at Mach numbers close to 1.0. In general, however, the distributions are the same; thus, the wing panel did not have a significant effect on the base pressure.

Variation of Average Pressure Coefficient for an

Assumed Jet Pressure Ratio Schedule

Figure 11 presents the variation of average base pressure coefficient with Mach number along an assumed jet pressure ratio schedule for the several configurations involving the $M_j = 2.0$ nozzles. The assumed jet pressure ratio schedule is typical for that proposed for $M_\infty = 3.0$ turbojet engines (ref. 1) and is shown in the upper left corner of each figure. Figure 11(a) compares the variations of $\bar{C}_{p,b}$ for the jet

pressure ratio schedule over the Mach number range investigated with
that obtained for the fixed area $M_j = 2.0$ nozzle operating at the
design pressure ratio of 7.8. This comparison shows that overexpanding
the jet flow produced more positive values of $\overline{C}_{p,b}$ than the fully
expanded nozzle up to a Mach number of about 1.15. Above this speed
the opposite was true. In figure 11(b) the effect of an inoperative jet
on the average base pressure coefficient is shown for the assumed jet
pressure ratio schedule. It will be seen in this figure that $\overline{C}_{p,b}$ was
greater (less negative) above $M_\infty = 0.9$ for the two-jet configuration
than for the three-jet configuration; below $M_\infty = 0.9$ the opposite was
true.

In figure 11(c) the variation of $\overline{C}_{p,b}$ with Mach number for the
schedule of jet pressure ratio is shown for the three basic nozzles.
As mentioned previously the 0.367-inch throat diameter was common to
these three nozzles. As can be seen in this figure only a small differ-
ence in $\overline{C}_{p,b}$ exists among the three nozzles over the speed range
of these tests. Therefore, the $M_j = 3.0$ nozzle would have the lowest
base drag because of the smaller base area for this configuration. These
data suggest that a configuration with a continuously variable nozzle
(for maintaining optimum thrust) would have about the same base pressure
coefficient as it would have with a fixed nozzle.

In figure 11(d) the effect of nozzle extension on the average base
pressure coefficient is shown for the assumed jet pressure ratio schedule.
The effect was very small below $M_\infty = 1.10$, the difference in $\overline{C}_{p,b}$
between the two configurations being about equal to the repeatability of
the data. Above $M_\infty = 1.15$ the effect of nozzle extension on the average
base pressure coefficient was greater with an increase in $\overline{C}_{p,b}$ of about
5 percent.

Variation of $C_{p,b}$ With Mach Number and Number of Jets

Data from the present investigation and from references 3, 5, 6,
and 7 are presented in the form of base pressure coefficient as a func-
tion of Mach number in figure 12. The data from references 3, 5, and 6
are for a cylindrical afterbody with a single jet exit. These data are
included to give a comparison between results for a single jet housed in
a cylindrical afterbody and multiple jets housed in a body of rectangular
cross section. The model configuration of reference 7 was similar to the
filled-base model $(M_j = 2.0)$ of the present tests. As noted in figure 12,
all data are presented for fully expanded nozzle conditions (ratio of jet
static pressure to free-stream static pressure of 1.0).

Relatively good agreement is noted at supersonic speeds between the single-jet, cylindrical afterbody configurations and the multiple-jet configuration. At transonic speeds, however, a similar comparison between single- and multiple-jet configurations with sonic nozzles shows only fair agreement. Although the data presented in figure 12 indicate that results from single-jet tests may approximate that which would be obtained for multiple-jet configurations, sufficient data are not available at the present time to substantiate a definite conclusion as to the applicability of data from single-jet tests to multiple-jet configurations. It is of interest to note in figure 12 that the variation of $C_{p,b}$ with Mach number obtained for the model with supersonic nozzles in the present tests appears to fair in rather smoothly with the variation of $C_{p,b}$ obtained for a similar model at higher speeds.

Calculated Base Drag and Nozzle Thrust for the

Three Basic Nozzles

In order to achieve a better understanding of the significance of the base pressure coefficients obtained in this investigation, calculations of base drag as a percentage of the nozzle thrust available were made for the three basic nozzles. The equations and methods used in these calculations are presented in the appendix and the results of the calculations are shown in figure 13. In this figure the ratio of base drag to the theoretical thrust of the three jets is presented as a function of jet pressure ratio for three values of M_∞. These data show that the base drag at transonic speeds may equal 50 percent of the theoretical engine thrust available within the operating range of typical Mach number 3 turbojet engines.

The calculated thrust used in the curves of figure 13 was found by assuming that the nozzles were operating with the jet flow attached to the nozzle walls at all times. This is probably not the case for the two supersonic nozzles at jet pressure ratios 60 percent or more below the design point. For the case where the nozzle flow separates from the wall of the nozzle, the resulting thrust would be greater than that calculated for the same nozzle with attached flow. However, the base drag would also be greater in this case since the nozzle wall downstream of the separation point would be subject to the subambient base pressure. Consequently, it is not readily possible to determine precisely the influence of nozzle flow separation on the curves of figure 13.

It will be noted in figure 13 that the performance, or drag-to-thrust ratio, of the $M_j = 3.0$ nozzle above $p_{t,j}/p_\infty = 4$ is better than that for the $M_j = 1.0$ and 2.0 nozzle so that the loss in thrust

due to overexpansion of the jet is more than offset by the reduced base drag. A similar result is noted in comparing the $M_j = 2.0$ nozzle with the $M_j = 1.0$ nozzle at jet pressure ratios below about 15.

This observation suggested that overexpansion of the jet in the case of a poor afterbody design might give better performance than operating the jet underexpanded or fully expanded. That is, the sum of base drag and thrust loss might be smaller for an overexpanded jet than for an underexpanded or fully expanded jet. It was reasoned that overexpanding the nozzle a reasonable amount would reduce the base drag, through reduction in base area, with only a small loss in thrust so that an overall gain in performance would result. In order to check this line of reasoning the computed results of figure 13 and a computed thrust loss were used to determine the sum of base drag and thrust loss for the $M_j = 1.0$ and 3.0 nozzles for comparison with the drag-to-thrust ratio of the $M_j = 2.0$ nozzle operating fully expanded. The thrust loss for the $M_j = 1.0$ and $M_j = 3.0$ nozzles was computed for the ideal jet pressure ratio of the $M_j = 2.0$ nozzle ($p_{t,j}/p_\infty = 7.8$). The sum of base drag and thrust loss obtained in this manner was 0.200 for nozzle 1, 0.105 for nozzle 2, and 0.214 for nozzle 3 at $M_\infty = 0.9$. At $M_\infty = 1.10$ the sum was 0.447, 0.350, and 0.365 for nozzles 1, 2, and 3, respectively. In a like manner, the results were 0.488, 0.401, and 0.442 at $M_\infty = 1.20$. These results show that the fully expanded nozzle configuration had the best performance but, when these results are plotted as a function of the ratio of nozzle exit area to the exit area of nozzle 2, it appears that the best performance point falls between an area ratio of 1.2 and about an area ratio of 1.5. Although a nozzle in this area-ratio range was not tested, the data of figure 11(c) tend to substantiate this observation. That is, the base pressure coefficient of a $M_j = 2.35$ nozzle, for instance, would be more positive than that for the $M_j = 2.0$ nozzle and, since the base area would be reduced with the larger nozzle, the base drag would be even further reduced. When the loss in thrust in overexpanding the jet flow to $M_j = 2.35$ is taken into account, it appears that the higher Mach number nozzle would have a lower sum of base drag and thrust loss than the $M_j = 2.0$ configuration. Although the overexpansion of the jet flow appears to give only a small gain in performance, the results indicate that it is preferred to an equivalent amount of underexpansion.

SUMMARY OF RESULTS

An investigation of the effect of side-by-side jets upon the base pressure of a rectangular cross-section body with a delta wing panel at Mach numbers of 0.6 to 1.27 yielded the following results:

1. Base pressure variation with jet pressure ratio for the model tested was similar to that obtained for single-jet exits in bodies of revolution in previous work. Peak negative base pressures of about 60 percent of the free-stream dynamic pressure were obtained at supersonic speeds on the model of this investigation.

2. The base pressure coefficient was increased (made less negative) by increasing the jet exit diameter for a given nozzle Mach number.

3. The effects on base pressure of extending the nozzle exits beyond the base a small amount and of closing off one jet were small and at some speeds the effect was within the repeatability error of the data.

4. Little difference in base pressure coefficient was found between nozzle design Mach numbers of 1, 2, and 3 with the same throat diameter for a jet pressure ratio schedule typical of turbojet engines operating in the speed range of these tests.

Langley Research Center,
    National Aeronautics and Space Administration,
        Langley Field, Va., March 25, 1959.

APPENDIX

THRUST AND DRAG EQUATIONS

The ratio of base drag to nozzle thrust was calculated in the following manner:

When it is assumed that there are no internal losses within the nozzle, the ratio of base drag to nozzle thrust may be written as

$$\frac{D_b}{F_j} = \frac{C_{D,b} q_\infty A_{max}}{3\left[w_j V_j + \left(p_j - p_\infty\right)A_j\right]} \tag{A1}$$

Since

$$w_j V_j = \left(\rho V A\right)_j V_j = 2q_j A_j \tag{A2}$$

equation (A1) may be written as

$$\frac{D_b}{F_j} = C_{D,b} \frac{A_{max}}{3A_j}\left[\frac{q_\infty}{2q_j + \left(p_j - p_\infty\right)}\right] \tag{A3}$$

Multiplying the numerator and denominator within the brackets of equation (A3) by $p_{t,o}/p_{t,o}$ and $p_{t,j}/p_{t,j}$, respectively, and dividing both numerator and denominator by p_∞ yields

$$\frac{D_b}{F_j} = C_{D,b} \frac{A_{max}}{3A_j} \frac{\left(\dfrac{q_\infty}{p_{t,o}}\right)\left(\dfrac{p_{t,o}}{p_\infty}\right)}{2\left(\dfrac{q_j}{p_{t,j}}\right)\left(\dfrac{p_{t,j}}{p_\infty}\right) + \left(\dfrac{p_j}{p_{t,j}}\right)\left(\dfrac{p_{t,j}}{p_\infty}\right) - 1} \tag{A4}$$

and since

$$\frac{A_{max}}{3A_j} = \frac{A_{max}}{3A_t} \frac{A_t}{A_j}$$

the final form for the drag-to-thrust ratio becomes

$$\frac{D_b}{F_j} = C_{D,b} \frac{A_{max}}{3A_t} \frac{A_t}{A_j} \frac{\left(\dfrac{q_\infty}{p_{t,o}}\right)\left(\dfrac{p_{t,o}}{p_\infty}\right)}{2\left(\dfrac{q_j}{p_{t,j}}\right)\left(\dfrac{p_{t,j}}{p_\infty}\right) + \left(\dfrac{p_j}{p_{t,j}}\right)\left(\dfrac{p_{t,j}}{p_\infty}\right) - 1} \qquad (A5)$$

In equation (A5) $A_{max}/3A_t$ is a constant for the three basic nozzles and is equal to 10.62. The base drag coefficient was computed from the known value of $\overline{C}_{p,b}$ (from fig. 5) and the ratio of base area to model cross-section area A_b/A_{max}, this ratio being equal to 0.695 for nozzle 1, 0.630 for nozzle 2, and 0.389 for nozzle 3. All other parameters in equation (A5), with exception of $p_{t,j}/p_\infty$, were obtained from the tables of reference 8, the free-stream Mach number and nozzle design Mach number being known.

The thrust loss due to overexpansion or underexpansion of the jet flow was computed from the following equation:

$$F_{j,loss} = 1 - \frac{F_j}{F_{j,i}} = 1 - \frac{w_j V_j + \left(p_j - p_\infty\right)A_j}{w_{j,i} V_{j,i}} \qquad (A6)$$

REFERENCES

1. Swihart, John M., and Nelson, William J.: Performance of Multiple Jet-Exit Installations. NACA RM L58E01, 1958.

2. Lord, Douglas R.: Longitudinal Stability Investigation of a Vertical-Take-Off-and-Landing Airplane Configuration With Simulated Jet Intake and Exhaust at Mach Numbers of 1.61 and 2.01. NACA RM L57K05, 1958.

3. Scott, William R., and Slocumb, Travis H., Jr.: Jet Effects on the Base Pressure of a Cylindrical Afterbody With Multiple-Jet Exits. NASA MEMO 3-10-59L, 1959.

4. Nelson, William J., and Scott, William R.: Jet Effects on the Base Drag of a Cylindrical Afterbody With Extended Nozzles. NACA RM L58A27, 1958.

5. Cubbage, James M., Jr.: Jet Effects on Base and Afterbody Pressures of a Cylindrical Afterbody at Transonic Speeds. NACA RM L56C21, 1956.

6. Bromm, August F., Jr., and O'Donnell, Robert M.: Investigation at Supersonic Speeds of the Effect of Jet Mach Number and Divergence Angle of the Nozzle Upon the Pressure of the Base Annulus of a Body of Revolution. NACA RM L54I16, 1954.

7. Swihart, John M., and Keith, Arvid L., Jr.: An Investigation of Clustered Jet-Exit Arrangements at Supersonic Speeds. NASA MEMO 5-11-59L, 1959.

8. Emmons, Howard W.: Gas Dynamics Tables for Air. Dover Publications, Inc., 1947.
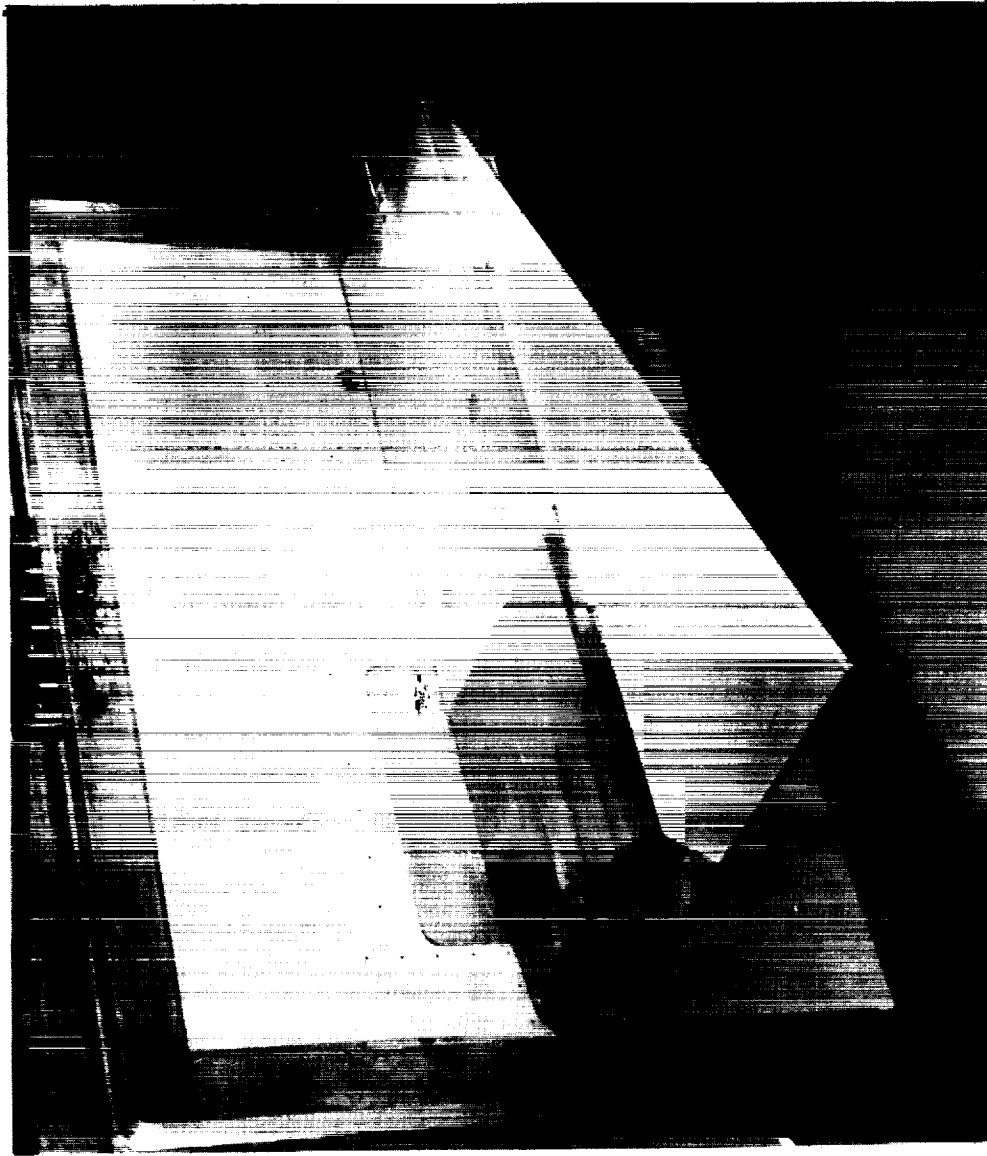
L-57-4858

(a) Photograph of model and mounting plate; $M_j = 3.0$ nozzles.

Figure 1.- Photographs and drawing of model.
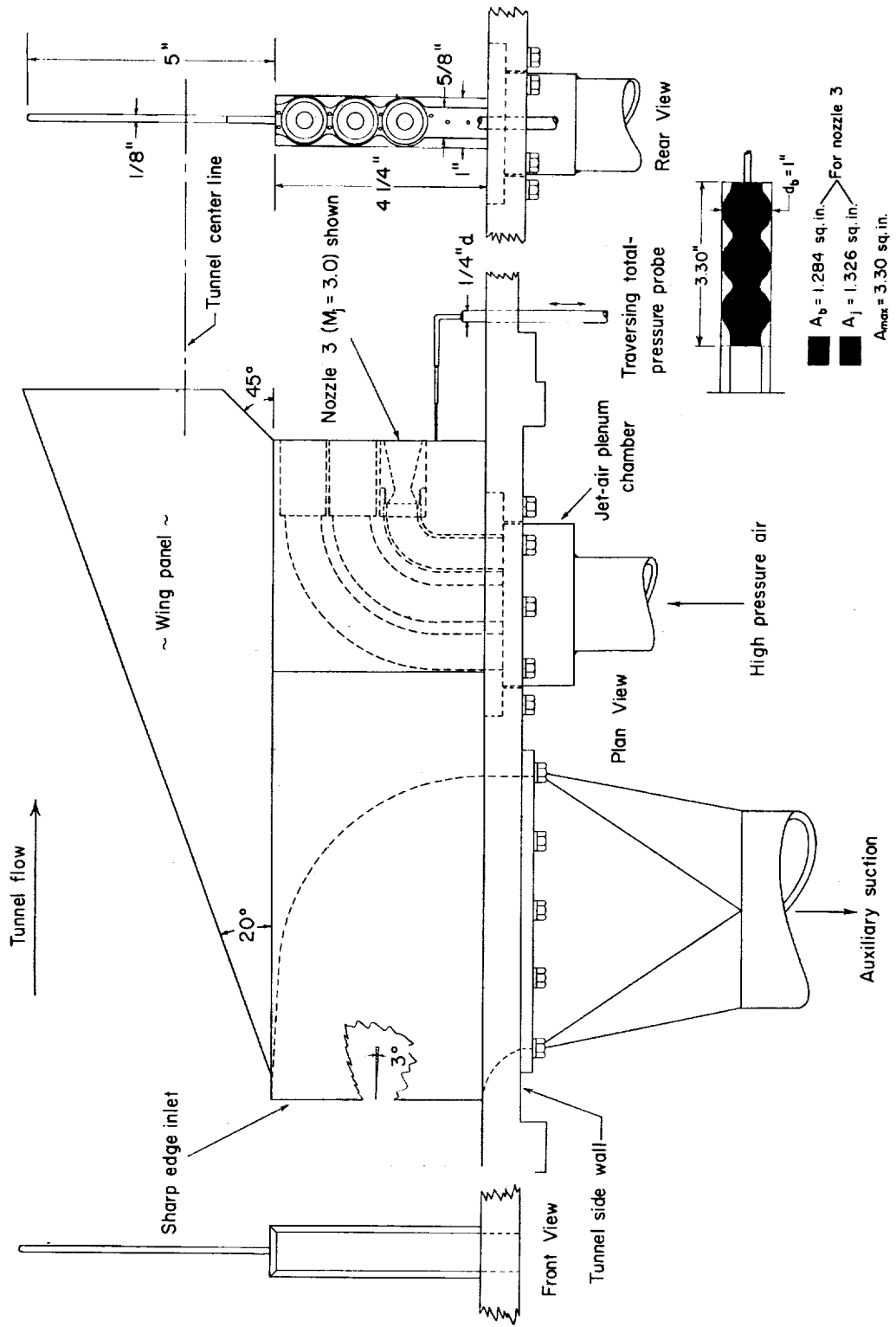
(b) Drawing of model.

Figure 1.- Continued.

18
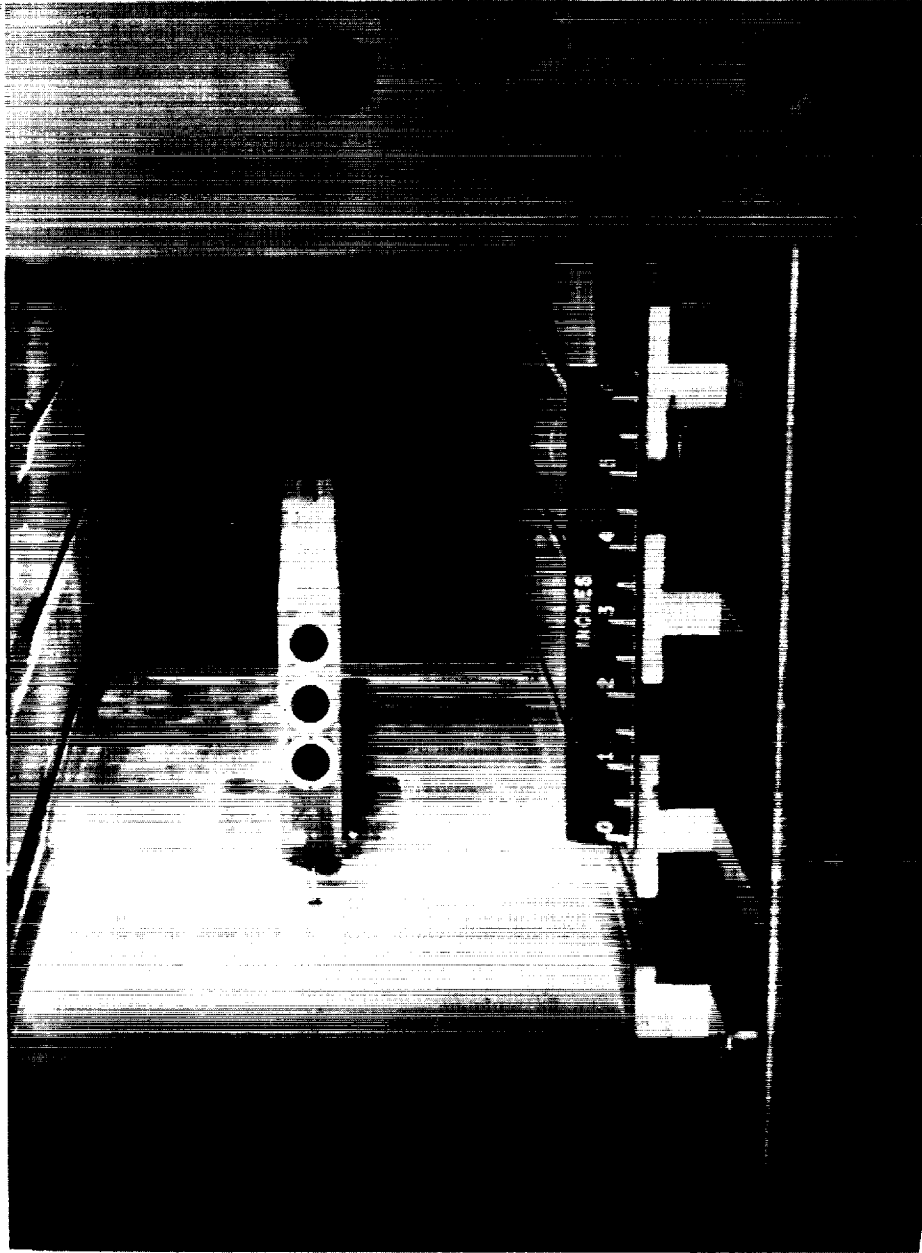
L-58-1354

(c) Upstream view of model from rear of tunnel; filled-base configuration, wing panel off, nozzle 2A.

Figure 1.- Concluded.
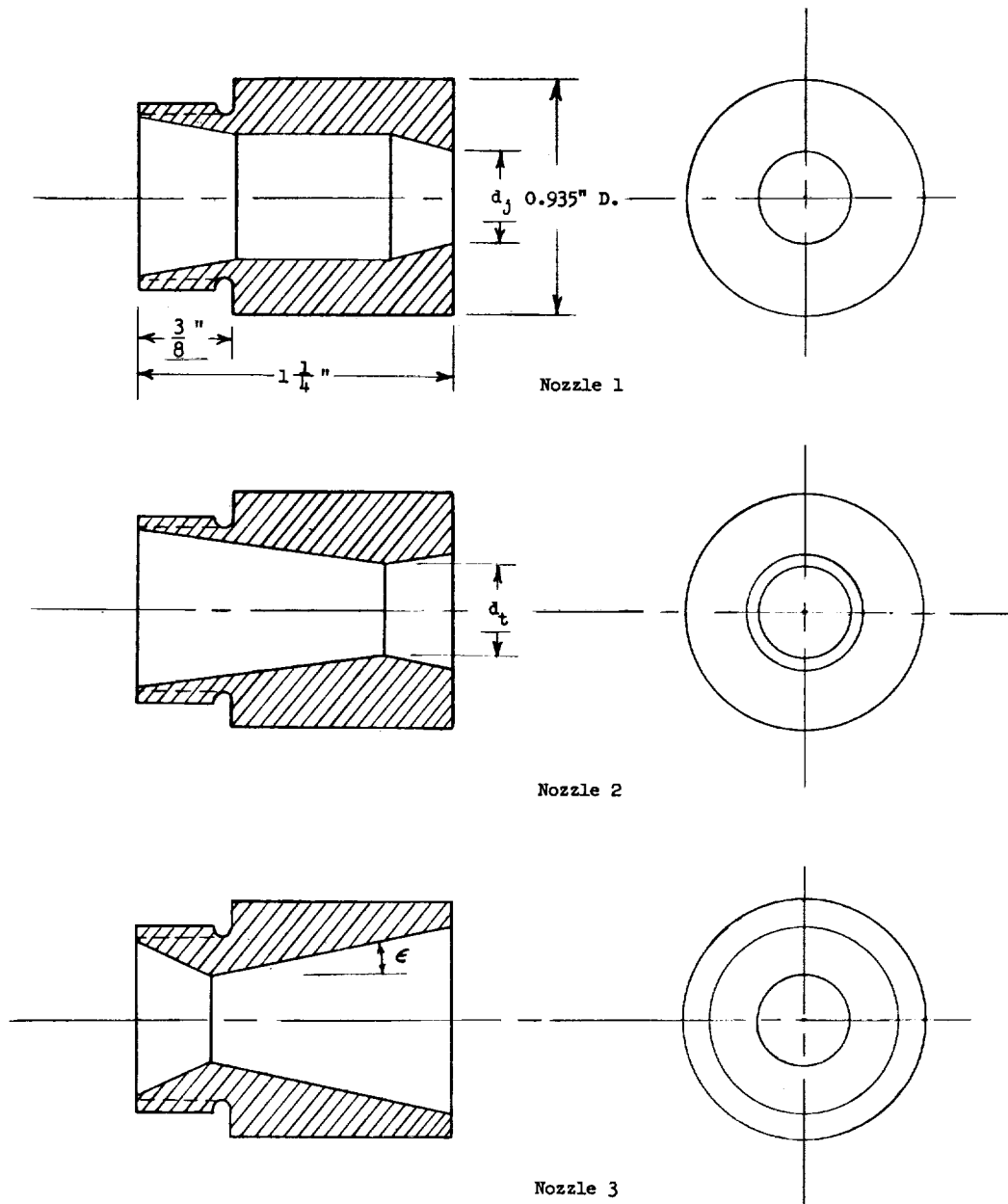
Nozzle	M_j	d_j	d_t	ϵ
1	1.0	0.364	0.364	-15°
1A	1.0	0.500	0.500	0
2	2.0	0.474	0.364	11.5°
2A	2.0	0.650	0.500	13°
3	3.0	0.750	0.364	11.5°

Figure 2.- Nozzle configurations investigated. All dimensions are in inches.

Jet air supply connection

Traversing probe actuator

Inlet-air removal connection

L-58-1353
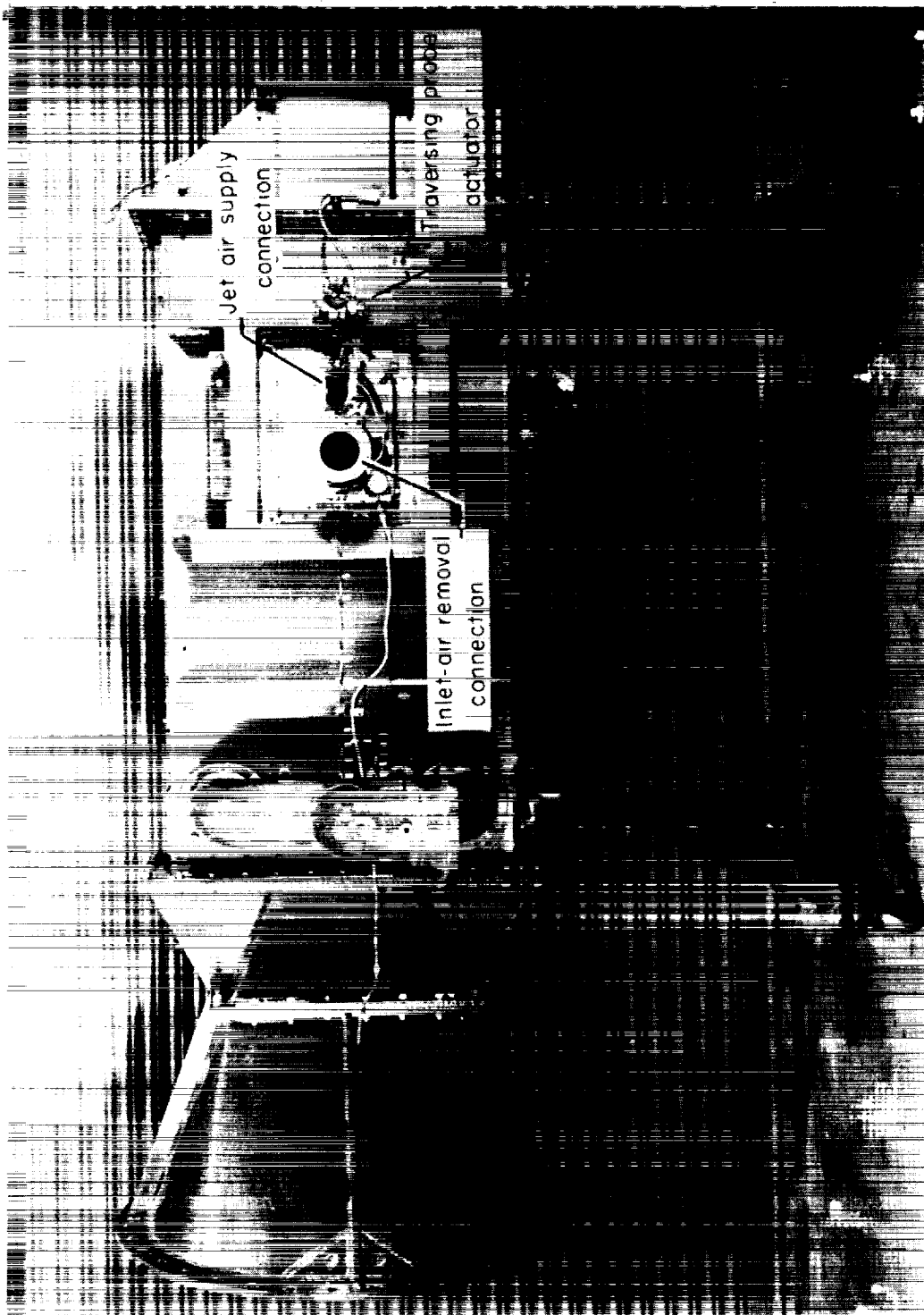
Figure 3.- Photograph of $8\frac{1}{2}$- inch by 12-inch slotted tunnel showing method of model installation.
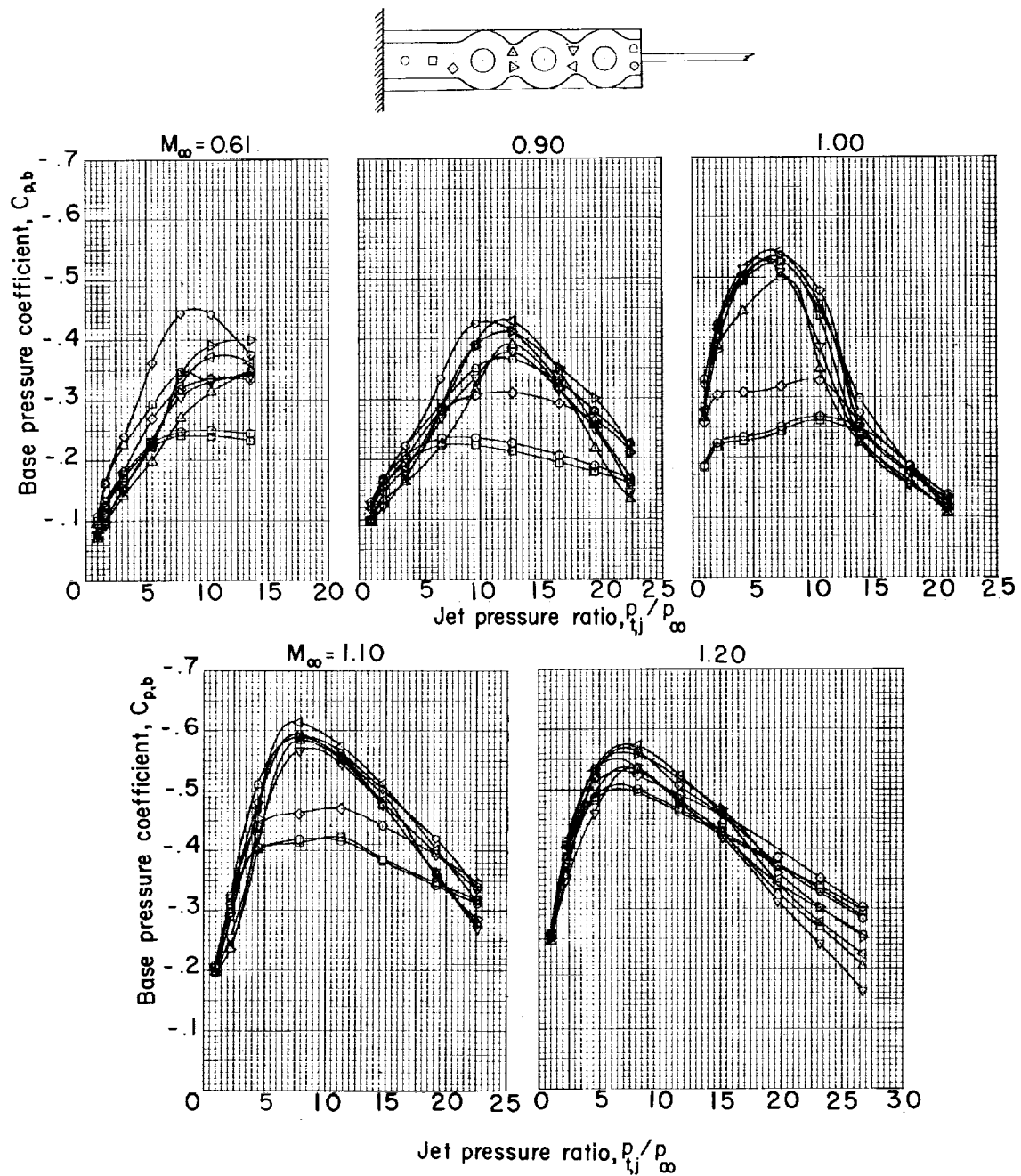
(a) $M_j = 1.0$.

Figure 4.- Variation of base pressure coefficient with jet pressure ratio for the individual base-pressure orifices.
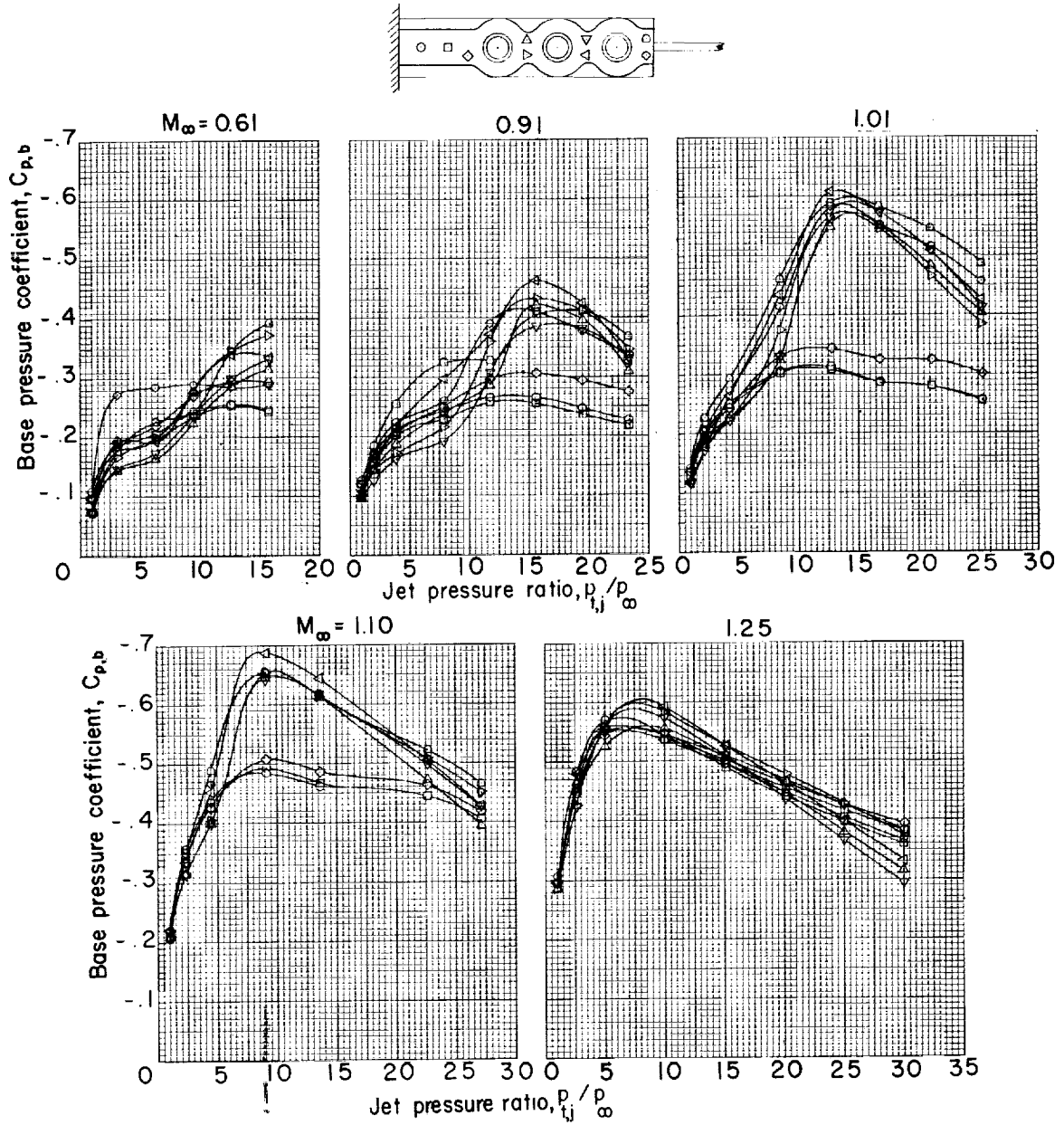
(b) $M_j = 2.0.$

Figure 4.- Continued.
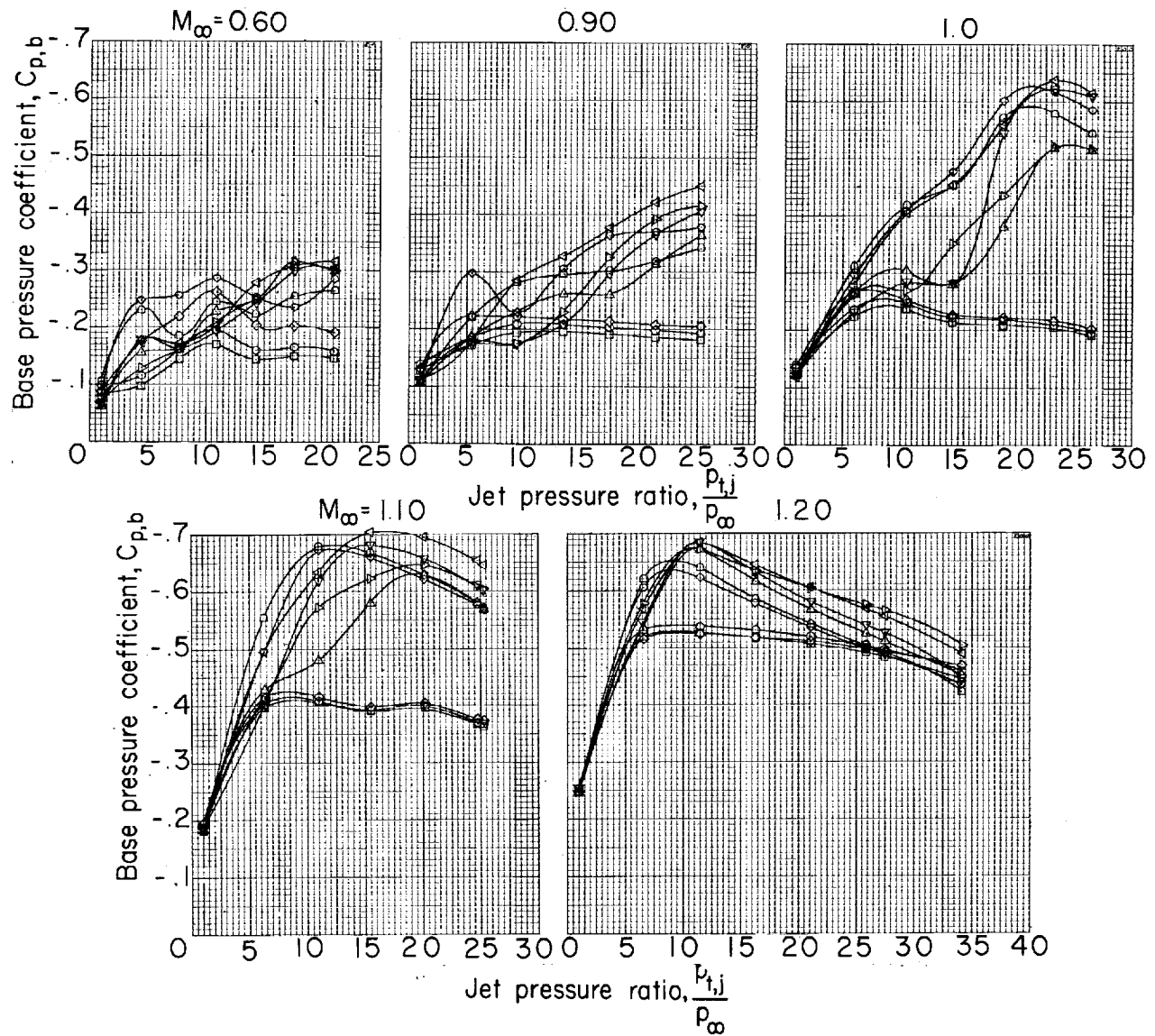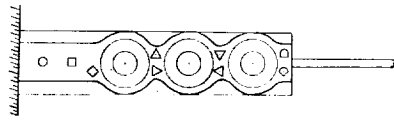
(c) M_j = 3.0.

Figure 4.- Concluded.

24
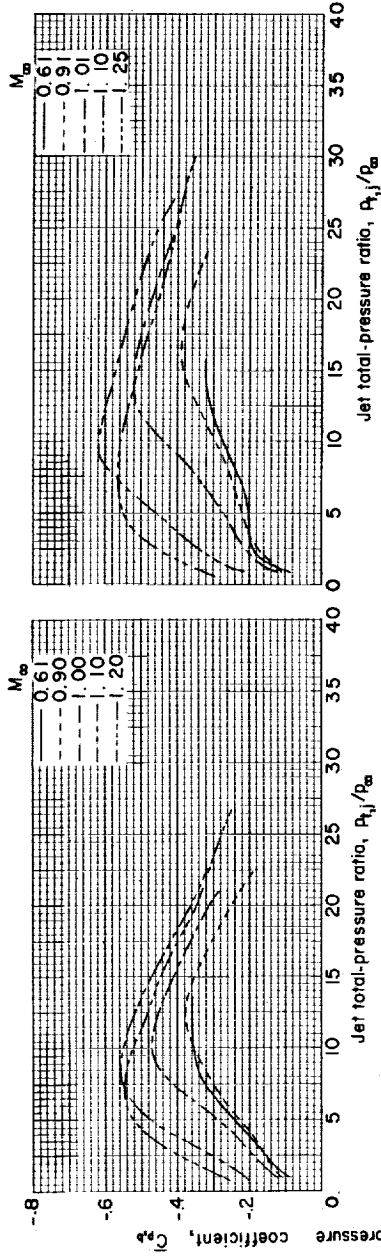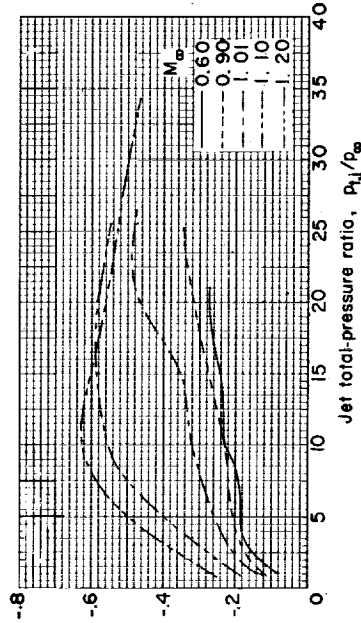
Figure 5.- Variation of average base pressure coefficient with jet pressure ratio for the three basic nozzles.
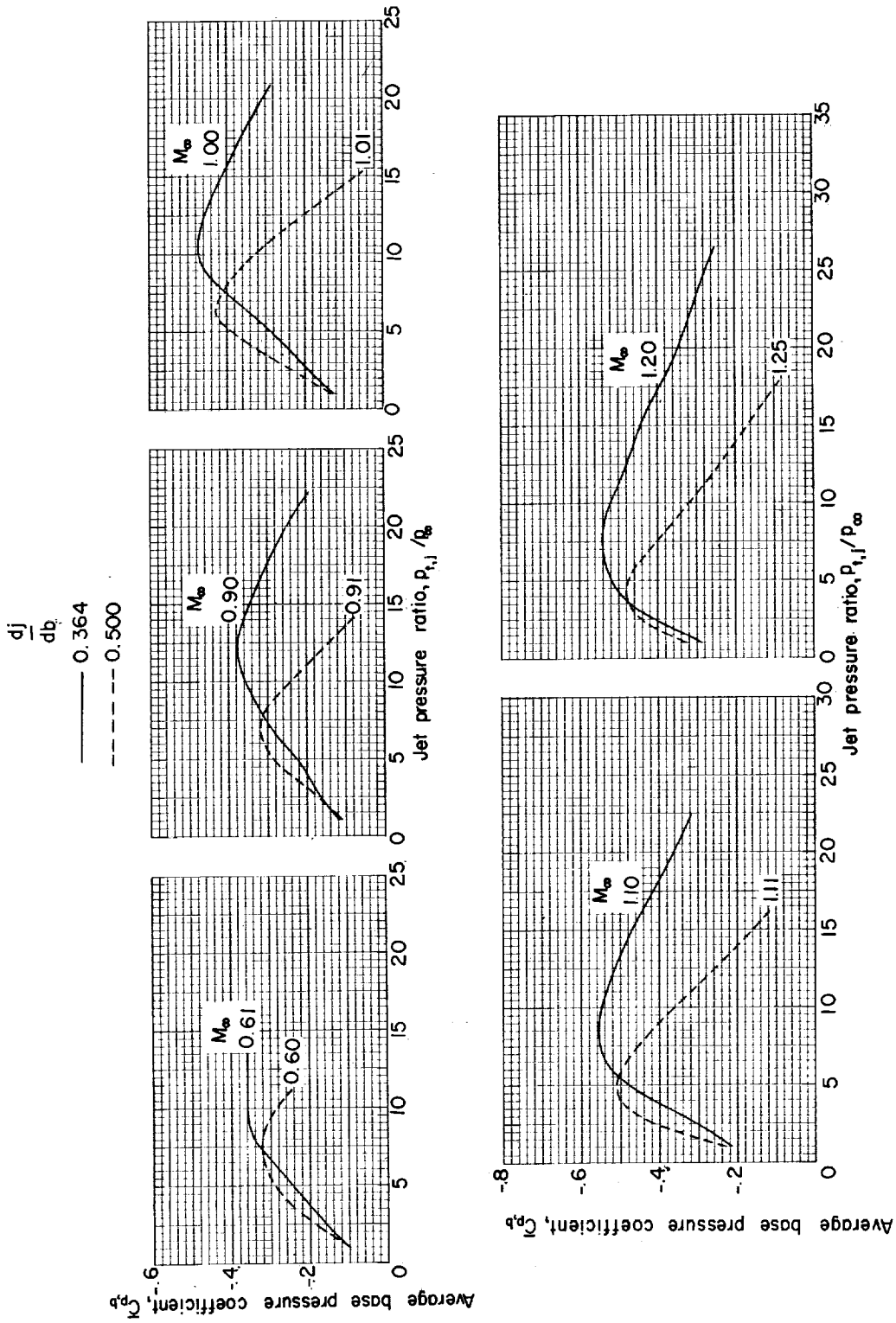
Figure 6.- Variation of average base pressure coefficient with jet pressure ratio showing effect of jet-to-base diameter ratio. $M_j = 1.0$.
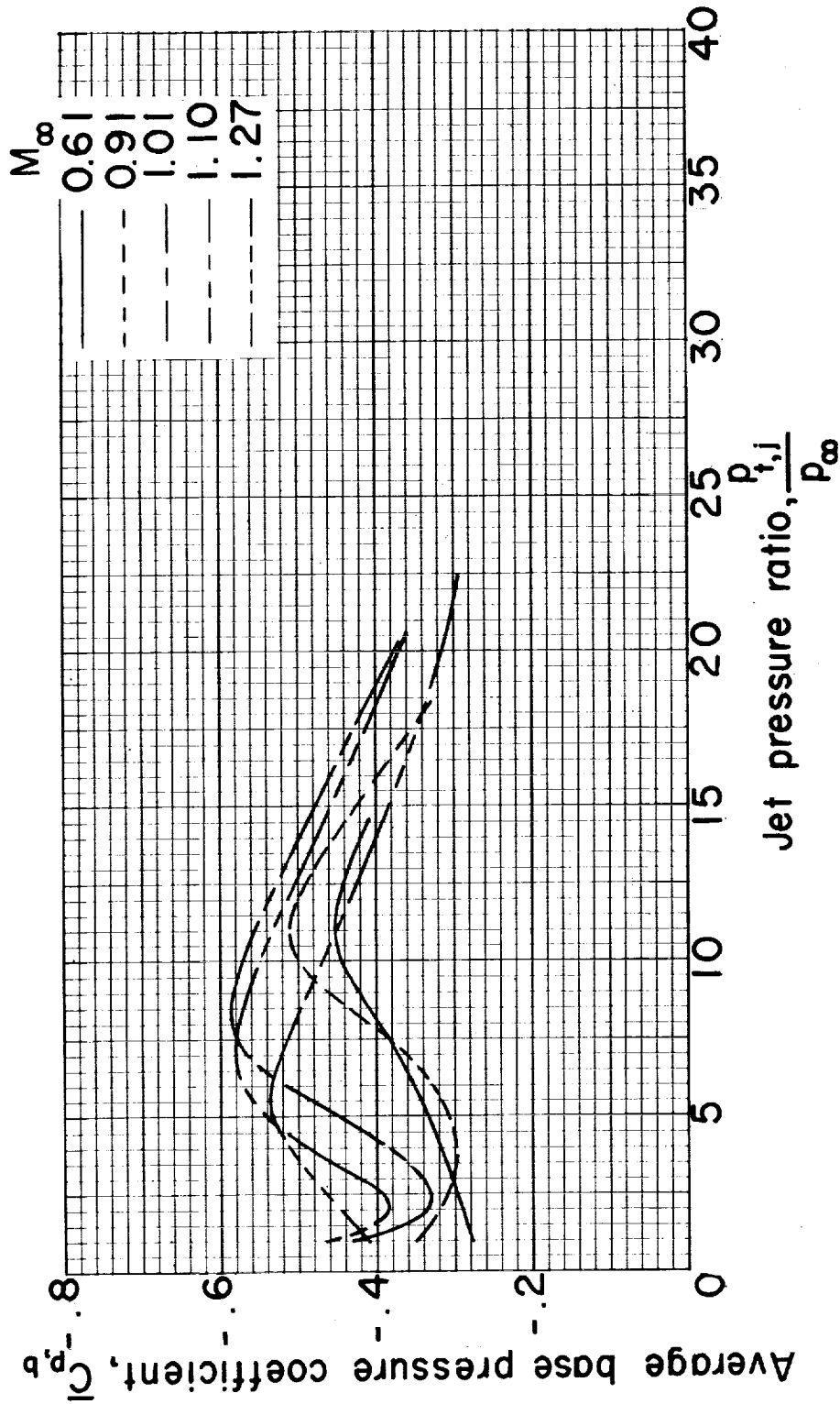
Figure 7.- Variation of average base pressure coefficient with pressure ratio for the filled-base configuration. $\frac{d_j}{d_b} = 0.64$; $M_j = 2.0$.

Average base pressure coefficient, $\bar{C}_{p,b}$

Jet pressure ratio, $\frac{p_{t,j}}{p_\infty}$

M_∞
0.61
0.91
1.01
1.10
1.27
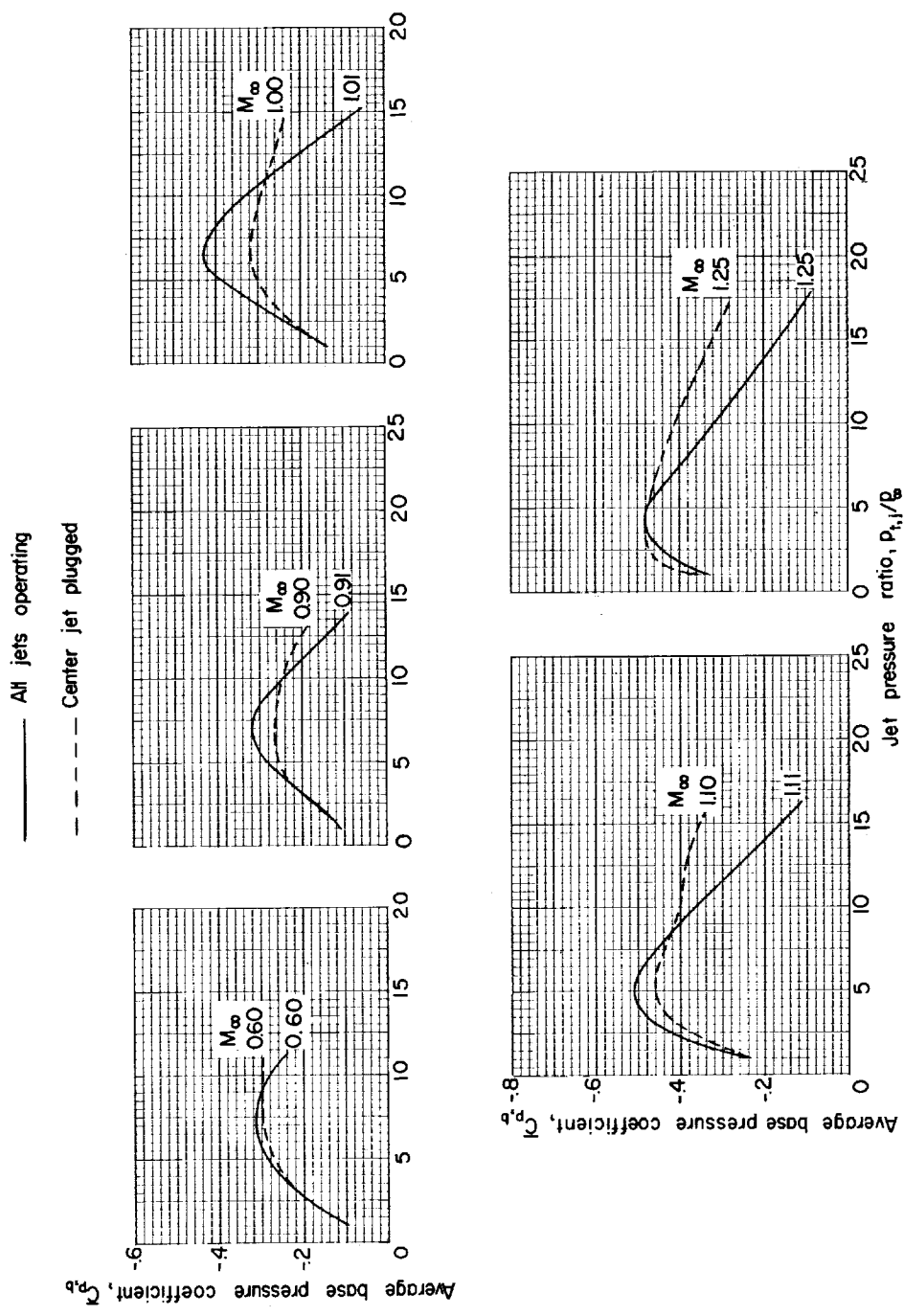
(a) $M_j = 1.0$; $\dfrac{d_j}{d_b} = 0.500$.

Figure 8.- Variation of average base pressure coefficient with jet pressure ratio showing effect of two-jet operation.

28
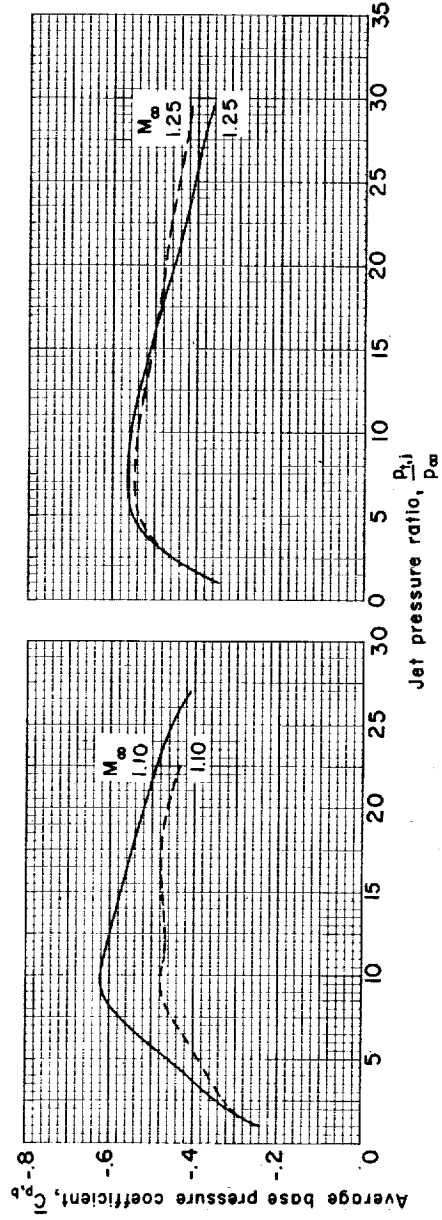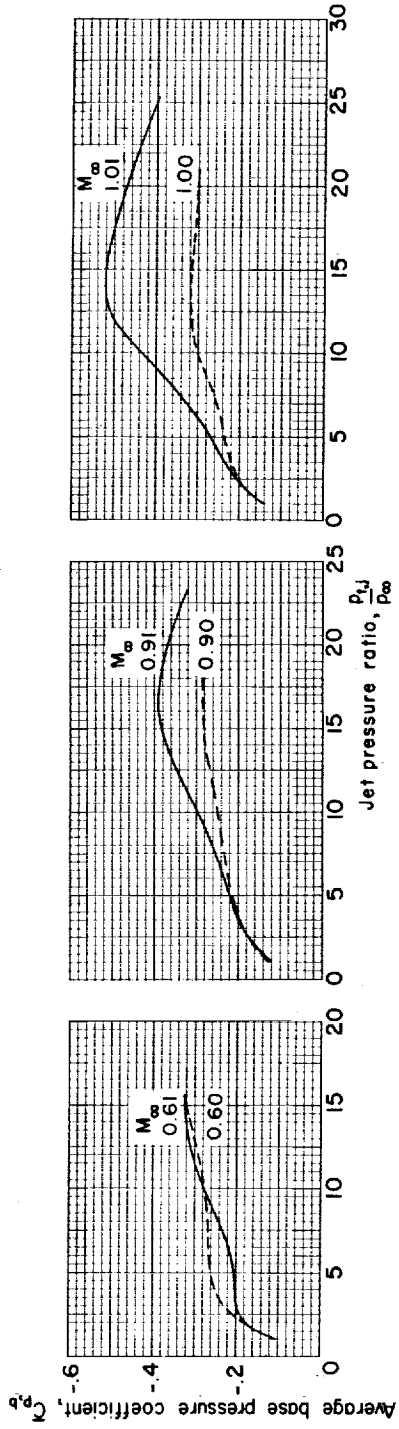
(b) $M_j = 2.0$; $\dfrac{d_j}{d_b} = 0.474$.

Figure 8.- Concluded.
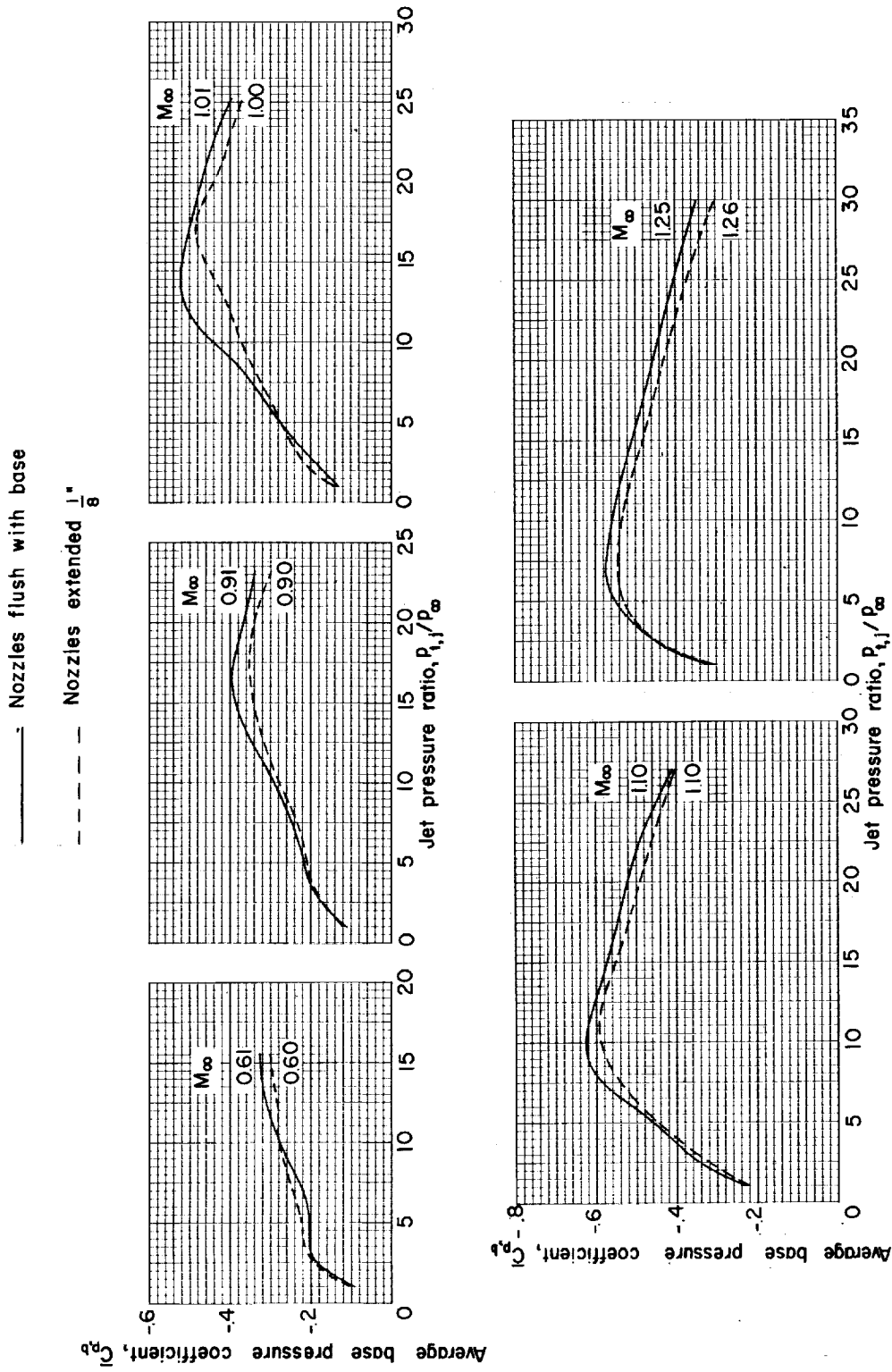
Figure 9.- Variation of average base pressure coefficient with jet pressure ratio showing effect of nozzle extension. $M_j = 2.0$; $\frac{d_j}{d_b} = 0.474$.

30
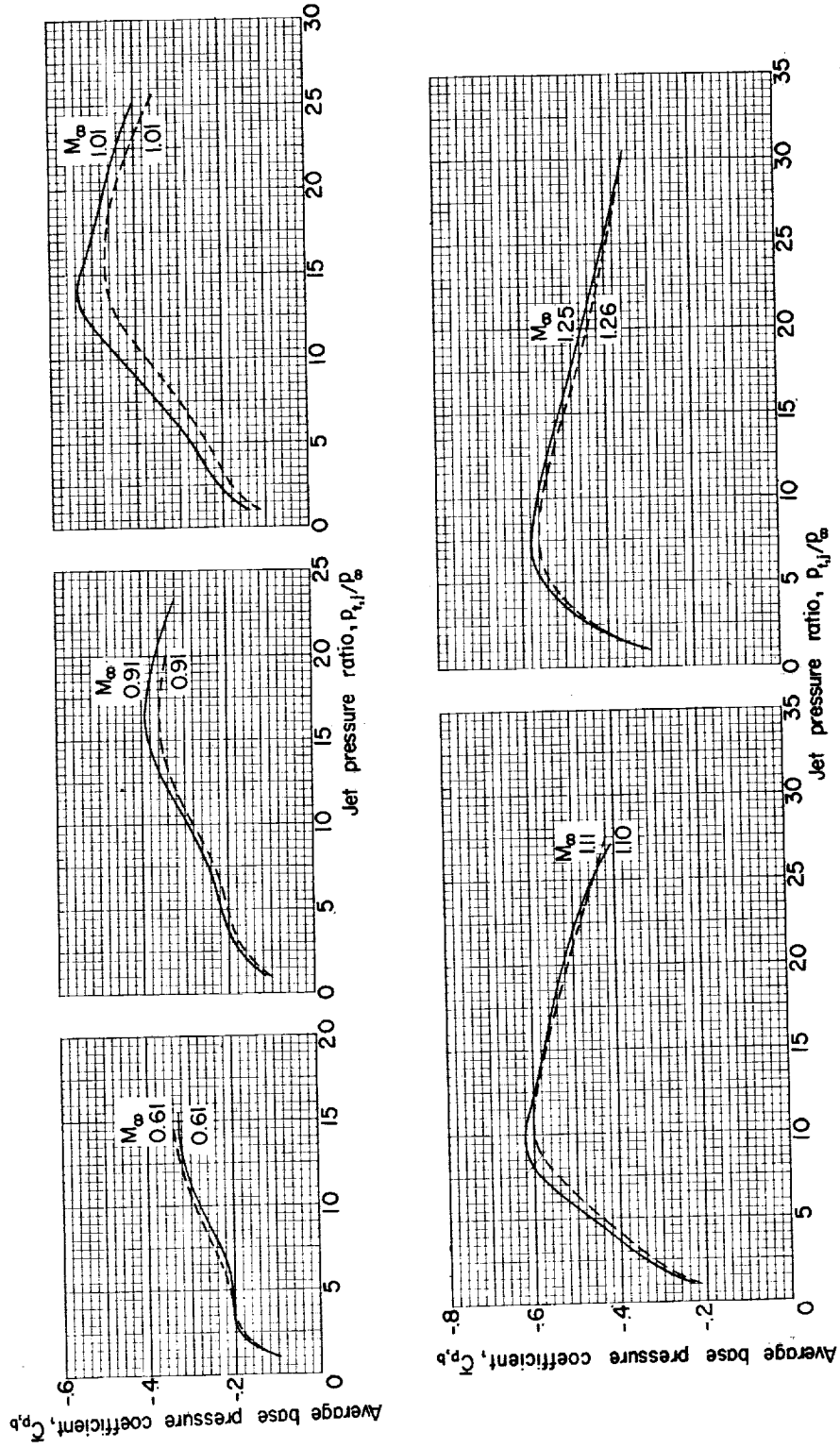
Figure 10.— Variation of average base pressure coefficient with jet pressure ratio showing effect of wing panel. $M_j = 2.0$; $\frac{d_j}{d_b} = 0.474$.
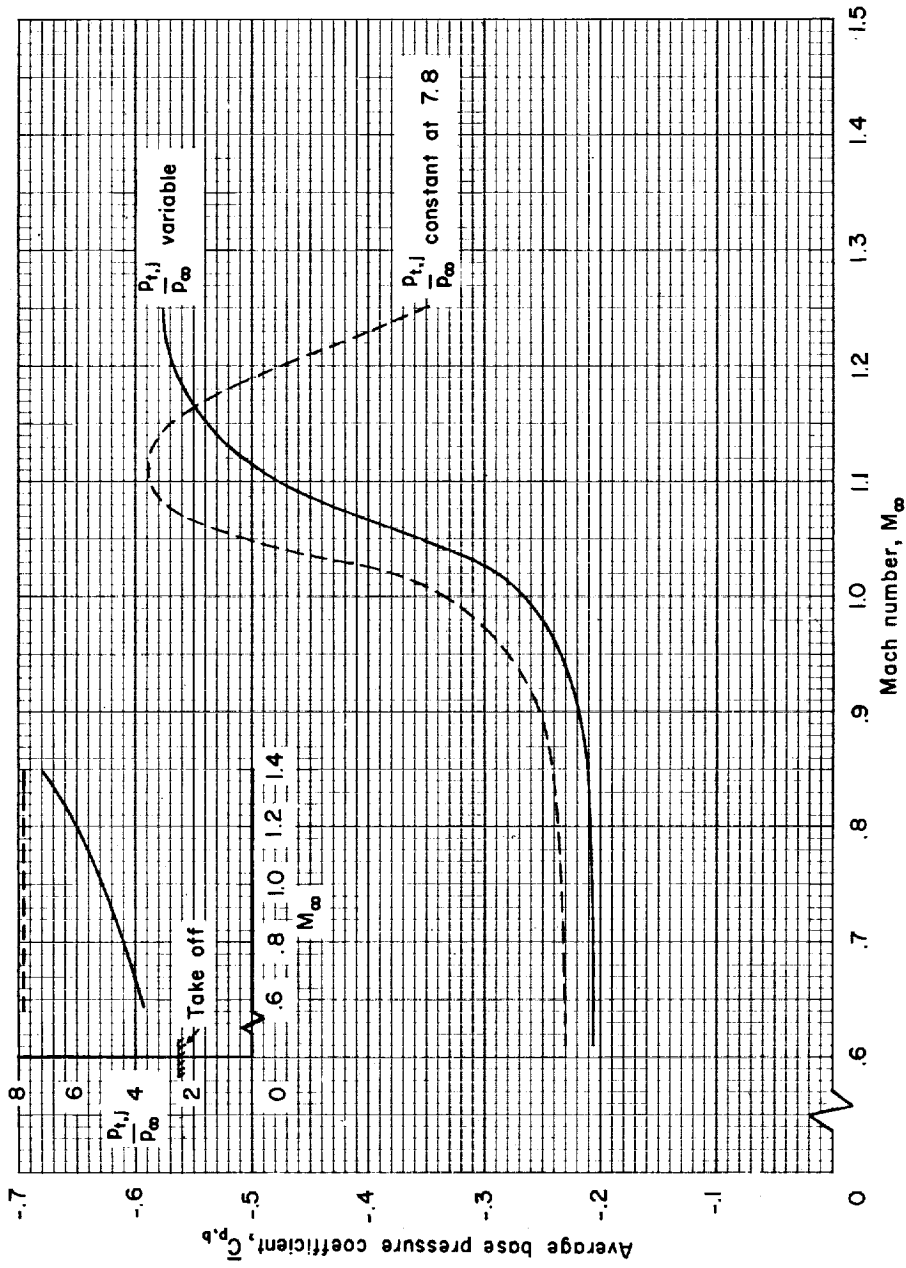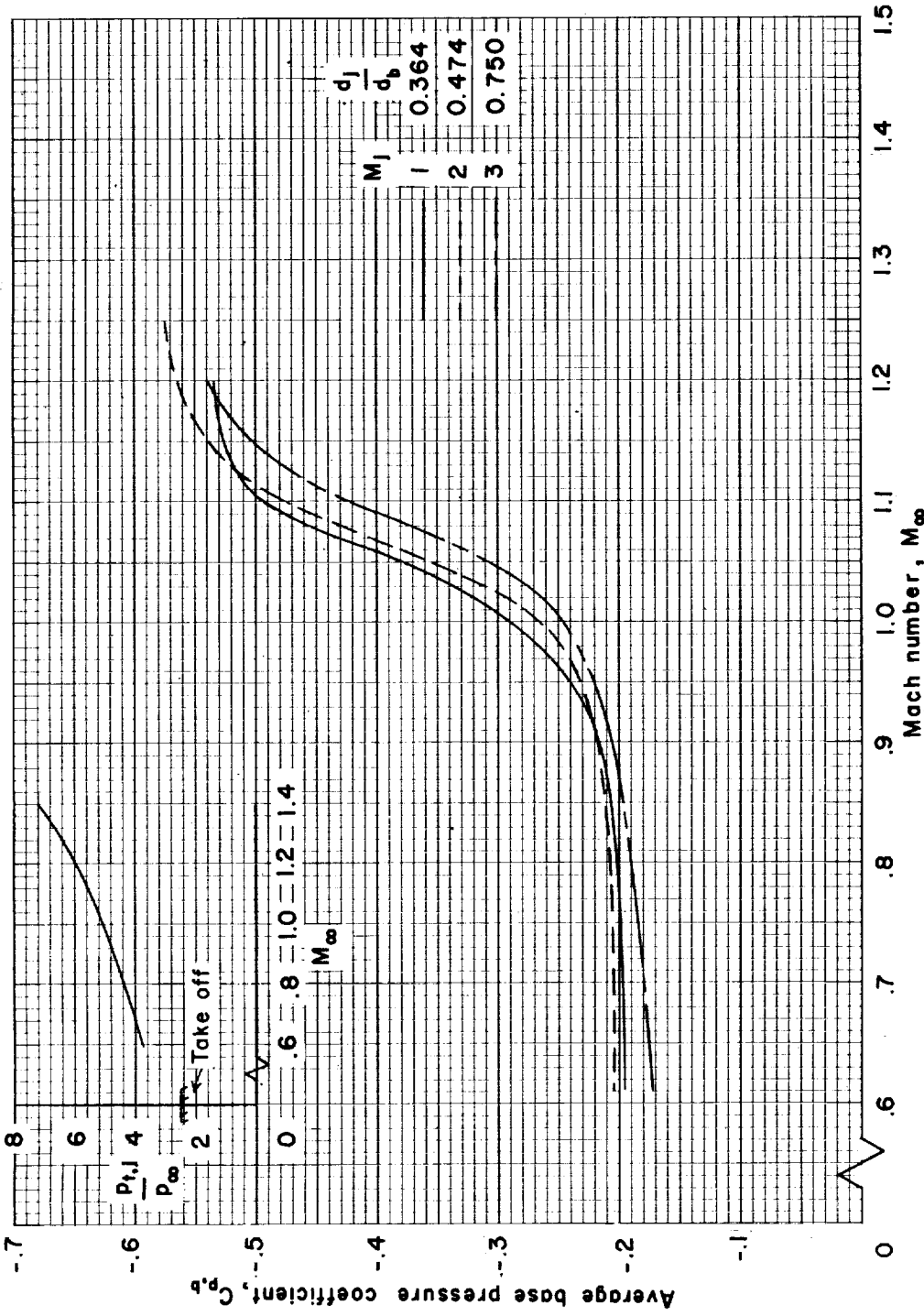
(a) Variation of $\overline{C}_{p,b}$ for variable and constant jet pressure ratios; $\dfrac{d_j}{d_b} = 0.474$.

Figure 11.- Variation of average base pressure coefficient with Mach number for an assumed engine pressure ratio schedule for the several configurations of the $M_j = 2.0$ nozzle.
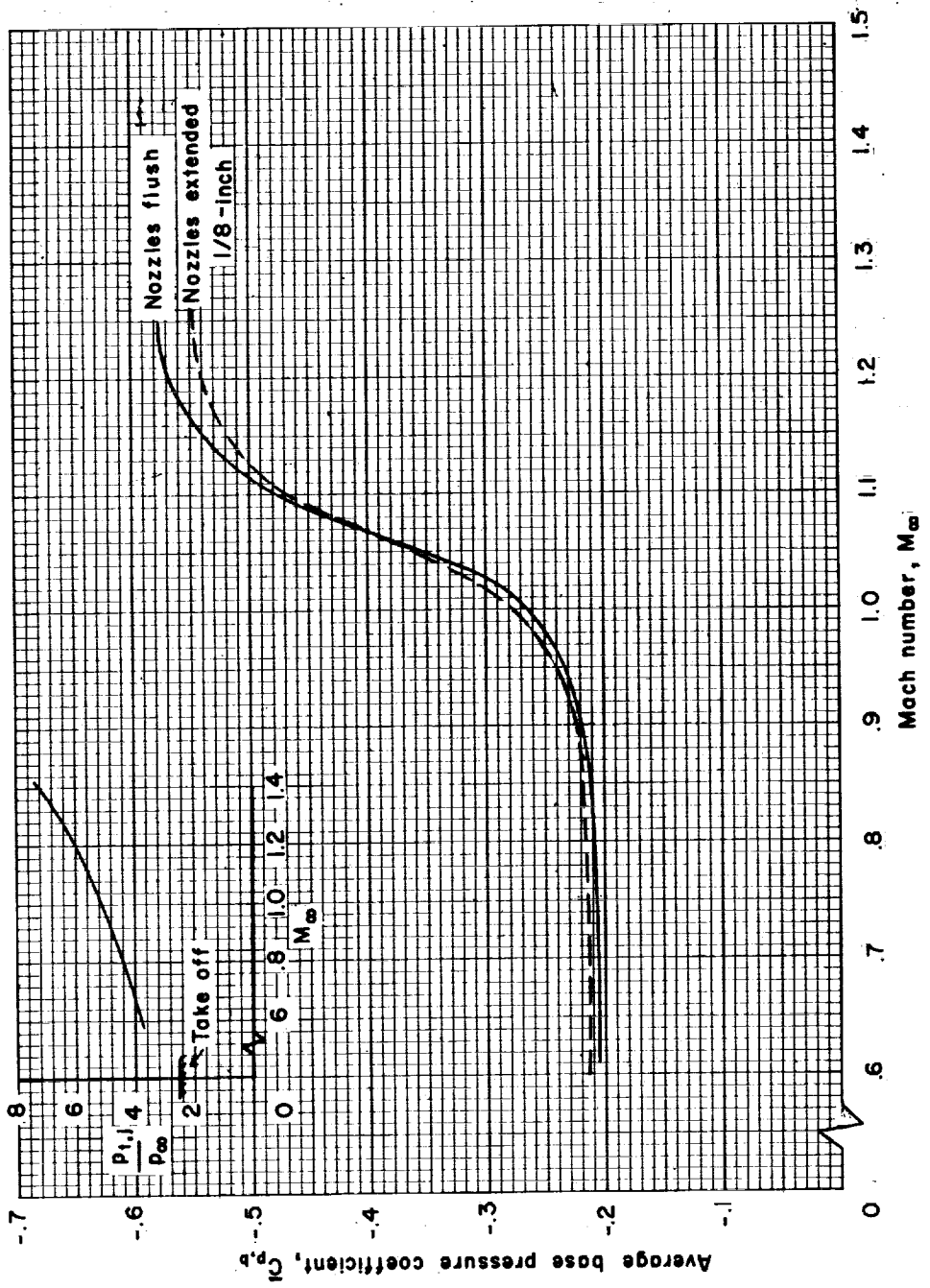
32
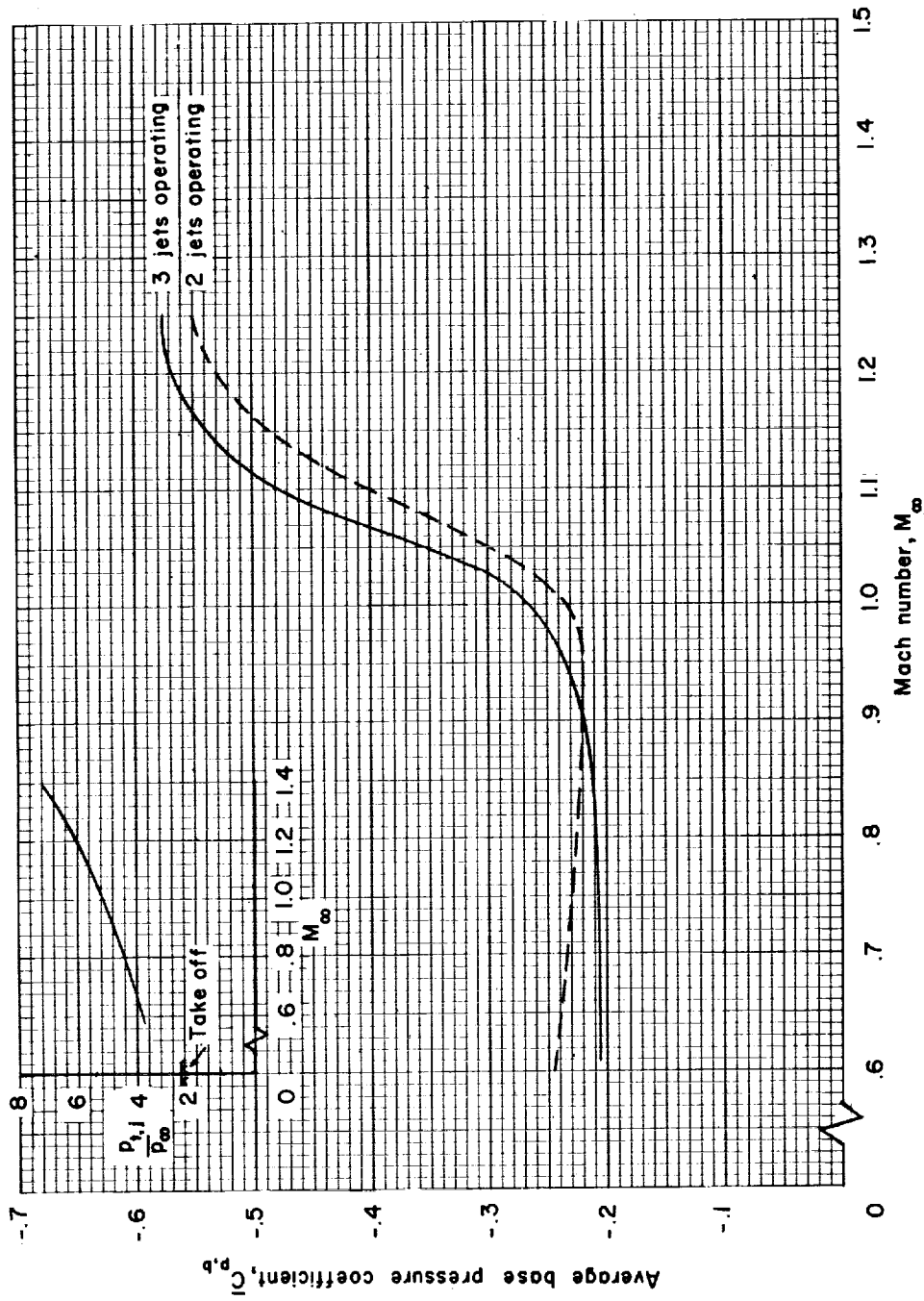
(b) Effect of one jet inoperative on $\overline{C}_{p,b}$; $\dfrac{d_j}{d_b} = 0.474$.

Figure 11.- Continued.

(c) Comparison of $\bar{C}_{p,b}$ variation with that for the $M_j = 1.0$ and 3.0 nozzles.

Figure 11.- Continued.

(d) Effect of nozzle extension on $\overline{C}_{p,b}$; $\frac{d_j}{d_b} = 0.474$.
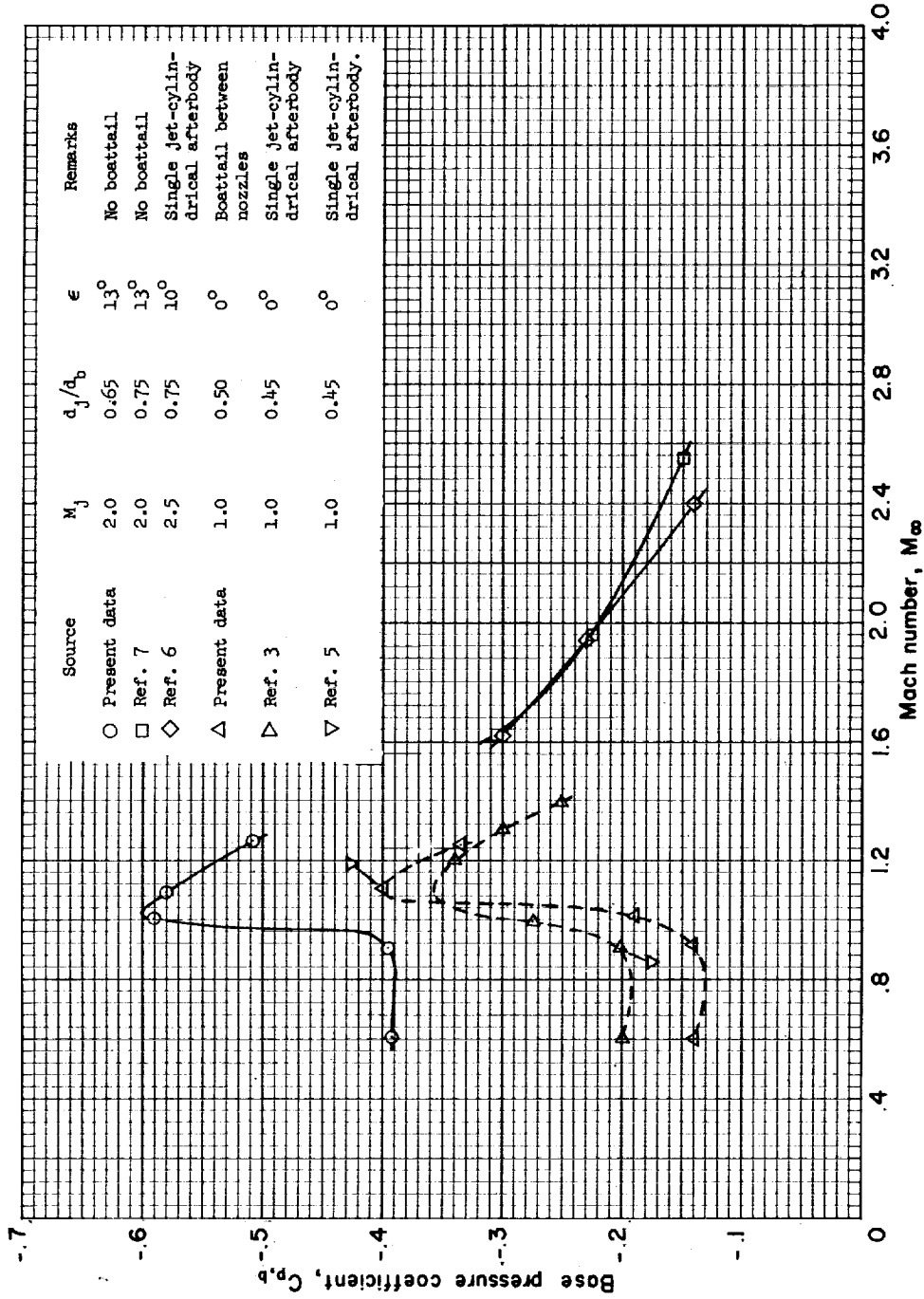
Figure 11.- Concluded.

Figure 12.- Variation of $C_{p,b}$ with Mach number of $\frac{p_j}{p_\infty} = 1.0$ for configurations of the present investigation, for similar configurations of higher Mach numbers, and for single-jet, cylindrical afterbody configurations at subsonic and supersonic speeds.
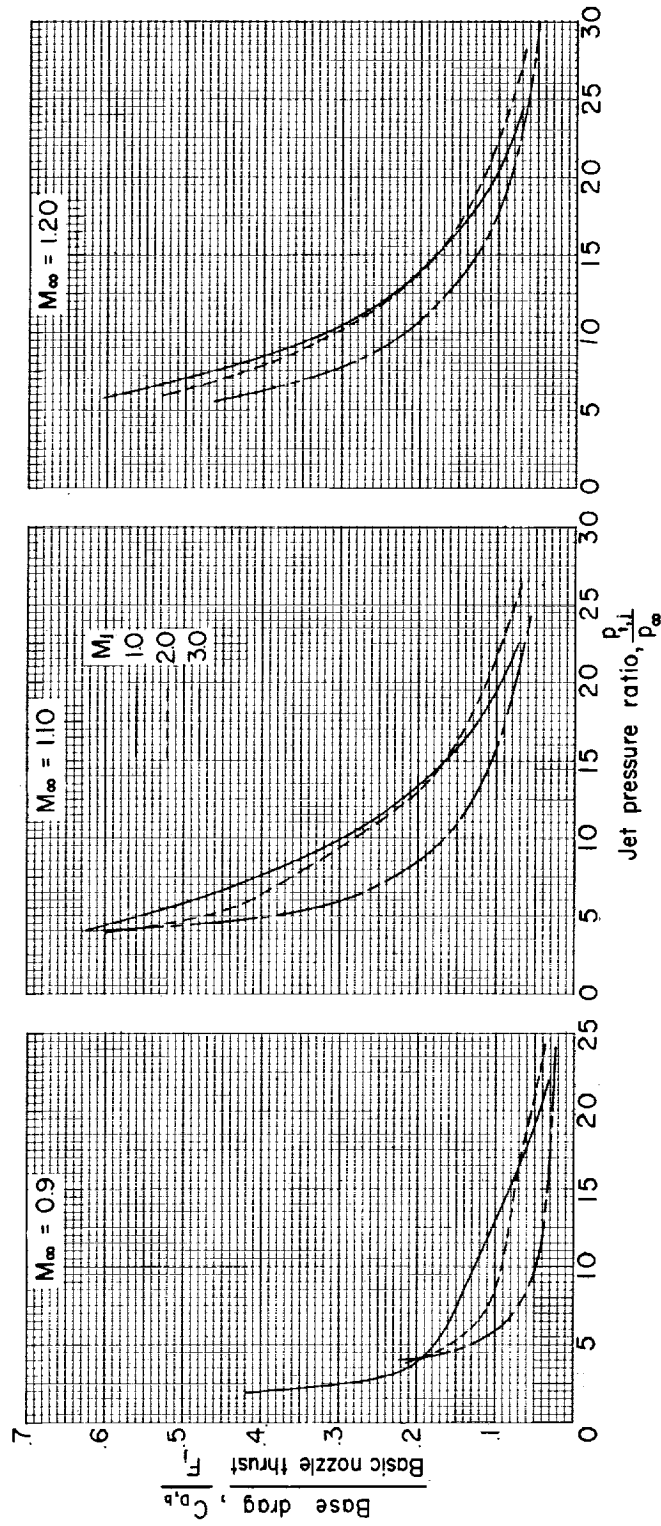
36

Figure 13. - Base drag as a percentage of the theoretical thrust available from the three basic nozzles.